

# Design Optimization of Permanent-Magnet Based Compact Transport Systems for Laser-Driven Proton Beams

1<sup>st</sup> Jared T. De Chant\*

Lawrence Berkeley National Laboratory  
Berkeley, CA USA  
jtdechant@lbl.gov

2<sup>nd</sup> Kei Nakamura

Lawrence Berkeley National Laboratory  
Berkeley, CA USA  
knakamura@lbl.gov

3<sup>rd</sup> Qing Ji

Lawrence Berkeley National Laboratory  
Berkeley, CA USA  
qji@lbl.gov

4<sup>th</sup> Lieselotte Obst-Huebl

Lawrence Berkeley National Laboratory  
Berkeley, CA USA  
lobsthuebl@lbl.gov

6<sup>th</sup> Samuel K. Barber

Lawrence Berkeley National Laboratory  
Berkeley, CA USA  
sbarber@lbl.gov

7<sup>nd</sup> Antoine M. Snijders

Lawrence Berkeley National Laboratory  
Berkeley, CA USA  
amsnijders@lbl.gov

8<sup>nd</sup> Thomas Schenkel

Lawrence Berkeley National Laboratory  
Berkeley, CA USA  
t\_schenkel@lbl.gov

9<sup>nd</sup> Jeroen van Tilborg

Lawrence Berkeley National Laboratory  
Berkeley, CA USA  
jvantilborg@lbl.gov

10<sup>th</sup> Cameron G. R. Geddes

Lawrence Berkeley National Laboratory  
Berkeley, CA USA  
cgrgeddes@lbl.gov

11<sup>th</sup> Carl B. Schroeder

Lawrence Berkeley National Laboratory  
Berkeley, CA USA  
cbschroeder@lbl.gov

12<sup>th</sup> Eric Esarey

Lawrence Berkeley National Laboratory  
Berkeley, CA USA  
ehesarey@lbl.gov

**Abstract**—Laser-driven (LD) ion acceleration has been explored in a newly constructed short focal length beamline at the BELLA petawatt facility (interaction point 2, iP2). For applications utilizing such LD ion beams, a beam transport system is required, which for reasons of compactness be ideally contained within 3 m. The large divergence and energy spread of LD ion beams present a unique challenge to transporting them compared to beams from conventional accelerators. This work gives an overview of proposed compact transport designs that can satisfy different requirements depending on the application for the iP2 proton beamline such as radiation biology, material science, and high energy density science. These designs are optimized for different parameters such as energy spread and peak proton density according to an application's need. The various designs consist solely of permanent magnet elements, which can provide high magnetic field gradients on a small footprint. While the field strengths are fixed, we have shown that the beam size and energy can be tuned effectively by varying the placement of the magnets. The performance of each design was evaluated based on high order particle tracking simulations of typical LD proton beams. A more detailed investigation was

carried out for a design to deliver 10 MeV LD accelerated ions for radiation biology applications. With these transport system designs, the iP2 beamline is ready to house various application experiments.

**Index Terms**—High intensity laser systems, Laser-plasma interactions, Laser-driven ion acceleration, Ion beam transport

## I. INTRODUCTION

Laser-driven (LD) ion acceleration has recently been explored in a newly constructed short-focal length beamline at the BELLA petawatt laser facility, named interaction point 2 (iP2) [1], which is available to users through LaserNetUS. In LD ion acceleration, a high intensity laser pulse ( $> 10^{21}$  W/cm<sup>2</sup>) interacts with a thin solid target, generates a plasma, and accelerates a large number of ions through various mechanisms. This acceleration technique differs from conventional RF cavity driven ion acceleration due to its high ion production ( $\sim 10^{13}$  ions per shot) and ultra short bunch length ( $\sim$ ps) [2]. These properties make LD ion beams attractive for certain applications, such as high dose rate radiobiology [3] and isochoric heating [4].

For the new iP2 area at BELLA, a compact proton beam transport system is needed for experiments exploring these applications. As different applications require different beam parameters, it is necessary to explore many different transport

The work was supported by Laboratory Directed Research and Development (LDRD) funding from LBNL provided by the Director, by the U.S. Department of Energy Office of Science, Offices of Fusion Energy Sciences and High Energy Physics under Contract No. DE-AC02-05CH11231, and by LaserNetUS (<https://www.lasernetus.org/>). J. T. De Chant was supported by the US Department of Energy, Office of Science, High Energy Physics under Cooperative Agreement award number DE-SC0018362.

\*Also at Michigan State University

configurations to better respond to users' needs. For example, proton therapy experiments require a uniform dose distribution over a relatively large area on target, while isochoric heating studies would more benefit from maximizing charge intensity on target.

Transporting LD ion beams has proved difficult due to the large divergence and energy spread of the beam. To accommodate these beams, high field gradient focusing elements have been used in the field, such as pulsed solenoids [5], [6] and active plasma lenses [7]–[9], and permanent magnet quadrupoles [10]–[13]. Due to available real estate surrounding the iP2 target chamber, the total length of transport from the ion source, including beam optics, diagnostics, and ion target, must be confined to 3 m. This constraint further complicates the design of the transport and is part of what motivated this study to focus only on the use of permanent magnet elements in the transport design, due to their compact size, high field strength, and lower cost.

This paper gives an overview of the methodology of designing the transport and highlights a few of the different configurations that were simulated to evaluate performance. This work allows the iP2 beamline to better respond to the needs of users and their various applications. A final configuration of the beam transport designed to deliver 10 MeV LD ion beams is also shown.

## II. DESIGN METHODOLOGY

### A. Beam parameters

In the simulations in the following sections, the properties of the beam coming out of the laser-plasma interaction region was modeled based on previous experiments and other LD ion accelerators. The initial beam was modeled as having a 2D Gaussian spatial distribution with a full-width-half-maximum (FWHM) beam size of  $100 \mu\text{m}$  and a beam divergence of  $450 \text{ mrad}$  [14], [15]. The angular divergence may depend on the particle energy [16] though here it was treated as constant. The energy spectrum was modeled as a Maxwell-Boltzmann distribution with a mean temperature of  $7 \text{ MeV}$  which is consistent with experimental ion acceleration results in the TNSA regime with on-target laser intensity of  $> 10^{20} \text{ W/cm}^2$  [17],

$$N(E)/\text{MeV} = 5 \times 10^{10} e^{-E/(7 \text{ MeV})}. \quad (1)$$

Particles with an initial divergence larger than the angular acceptance of the first magnet are neglected for the rest of the calculations but are used to estimate the collection efficiency. After the initial beam is prepared, the trajectory is simulated through a transport configuration. The performance of each transport design was then evaluated by estimating the peak density, energy acceptance, and beam spot size of the output beam.

### B. Permanent magnet optical elements

This study uses permanent magnet optical elements to focus and deflect the ion beam. Sets of permanent magnets with

specific magnetization vectors can be arranged in a Halbach array [18] to achieve the same field profiles seen in typical electromagnetic optical elements (e.g. dipoles, quadrupoles, and sextupoles) but with higher fields. In general, permanent magnet quadrupoles can achieve gradients of  $100\text{s T/m}$  while their normal conducting electro-magnetic counterpart is typically limited to  $1 \text{ T/m}$ . Superconducting magnets [19] produce a very strong field gradient but run the risk of quenching from being so close to the interaction point.

Permanent magnet quadrupoles (PMQs) are able to achieve this field strength with a relatively large bore ( $20 \text{ mm}$ ) which is important as a large bore leads to a larger admittance. And as the applications for LD accelerated beams generally require a large beam current, maximizing collection efficiency is crucial for the transport design.

The magneto-static simulation code RADIA [20] was used to design the PMQs and an example geometry is shown in Fig. 1. The magnets were based off an 8-azimuthal-segment Halbach array with  $1.29 \text{ T}$  of the bulk magnetisation  $B_r$ . This configuration is readily achievable for commercial vendors, and this bulk magnetisation level is typical for a N40 grade Nd-FeB magnet, which is also commercially available at relatively low cost. A list of properties of the PMQs used in the design work is shown in Table I. The use of permanent magnet dipoles (PMDs) was also investigated as they are energy dispersive and thus can be used to deflect ions of undesired energy off of the main beam path. The properties of the PMDs used in this work are shown in Table II.

Permanent magnet optical elements are not easily tunable as their field gradients are fixed after fabrication. However, the properties of the beam can still be tailored to suit the needs of applications. Varying the number of magnets and their relative spacing allows for some flexibility in the beam profile and energy distribution.

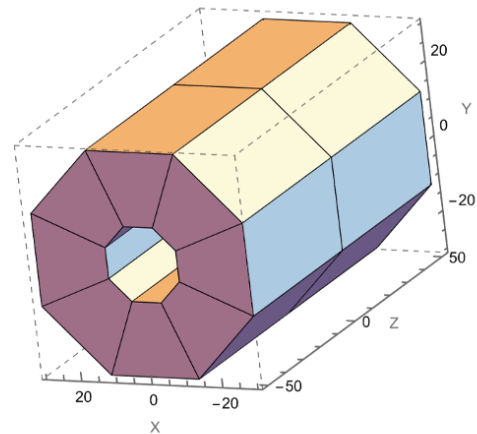


Fig. 1. Visualization of permanent magnet quadrupole. The parameters are described in Table I.

TABLE I  
PROPERTIES OF THE PERMANENT MAGNET QUADRUPOLES

PMQ parameters	
Inner radius	10 mm
Outer radius	30 mm
Bulk magnetisation $B_r$	1.29 T
Effective magnetic field at tip $B_{tip}$	1.16 T

TABLE II  
PROPERTIES OF THE PERMANENT MAGNET DIPOLES

PMD parameters	
Half gap	10 mm
Bulk magnetisation $B_r$	1.29 T
Effective magnetic field $B_D$	0.89 T

### C. Simulation

The design of each transport configuration was done using COSY INFINITY [21] (COSY), an arbitrary order beam dynamics simulation and analysis code. COSY allows for the study of accelerator lattices, spectrographs, beam transports, electron microscopes, and many other devices. With differential algebraic techniques, it calculates Taylor maps, a representation of the motion of charged particle in an arrangement of electromagnetic fields, to arbitrary order. Applying the map,  $M$ , of some transport lattice to the phase-space vector describing the initial beam distribution,  $\vec{z}_0$ , produces an estimate of the phase-space vector of the beam after having passed through the transport  $\vec{z}_f$ .

$$\vec{z}_f = M(\vec{z}_0). \quad (2)$$

In COSY, each configuration of optical elements was optimized to achieve either point-to-point focusing or collimation at the target location. The COSY output maps were used to evaluate a system's angular acceptance and transmission efficiency. In order to analyze the performance of the transport systems with arbitrary input ion beams, a home-made MATLAB script was written. This script applies the COSY map to the phase-space vectors of a large number of particles to simulate their trajectories and calculate macro-properties of the beam, such as the charge density profile and energy spread.

Due to the large energy spread and divergence of the initial beam, simulations had to be performed at 3rd order or above to account for spherical and chromatic aberrations inherent to the charged particle optics that would not be included in a linear mapping.

## III. RESULTS

### A. Comparing doublet, triplet, and quartet configurations

Various configurations of transport elements were investigated to achieve point-to-point focusing of a 30 MeV ion beam. This was done to explore the general costs and benefits of varying the number of magnets. A selection of the designs

are shown here, referred to as the doublet, triplet, and quartet corresponding to the number of PMQs present in the configuration. The horizontal and vertical trajectories of particles with the maximum initial angle that is accepted by the transport are shown for each of the configurations in Fig. 2. The different colors show the trajectories of similar particles with energies 20% above (blue) and 20% below (red) the nominal beam energy of 30 MeV (green). Real quadrupoles focus off-energy particles to different focal positions from the nominal focus. This can only be seen in higher order expansions of the quadrupole focusing kick.

The performance of each configuration was evaluated by estimating the collection efficiency  $\eta$ , peak proton density  $n_{pk}$ , momentum acceptance  $\delta E$ , and FWHM beam size in  $x$  ( $\sigma_x$ ) and  $y$  ( $\sigma_y$ ). The results for the selection of configurations is shown in Table III to compare.

TABLE III  
SIMULATION RESULTS OF COLLECTION EFFICIENCY  $\eta$ , PEAK PROTON DENSITY  $n_{pk}$ , ENERGY ACCEPTANCE  $\delta E$ , AND FWHM BEAM SIZE IN  $x$  ( $\sigma_x$ ) AND  $y$  ( $\sigma_y$ ) PROPAGATED THROUGH THE DIFFERENT PMQ CONFIGURATIONS INVESTIGATED IN THIS WORK.

	$\eta$ (%)	$n_{pk}$ ( $10^9/\text{mm}^2$ )	$\delta E$ (MeV)	$\sigma_x$ (mm)	$\sigma_y$ (mm)
Doublet	2.2	18	0.75	0.84	0.03
Triplet	2.5	25	0.85	0.13	0.17
Quartet	1.3	6.6	1.2	0.34	0.35

The simplest configuration is a doublet, or two quadrupole magnets in succession with drift space in between. Two are required at minimum as quadrupole magnets are simultaneously focusing in one plane and defocusing in the other but can be combined together to create overall focusing. As seen in Table III, the doublet configuration has a high collection efficiency (>2%) but produces a very asymmetric beam shape on the target. This configuration may be sufficient for applications that mostly require a high beam intensity such as isochoric heating.

Adding a third magnet improves the collection efficiency, charge density, and symmetry of the beam spot as the extra magnet adds further control over the beam. This configuration may be sufficient for most applications as it performs moderately well in all areas.

A fourth magnet reduces the overall acceptance of the transport and thus reduces the collection efficiency and charge density. However, the beam spot is nearly perfectly symmetric and the energy acceptance is the highest of the three. This configuration may be more suited for applications such as radiobiology as it would produce a more controlled dose deposition.

### B. Energy tunability

The main energy of the beam delivered onto target can be tuned in a few different ways. For each of the configurations, the drift lengths between the magnets can be varied so that the nominal beam energy is focused at the target location.

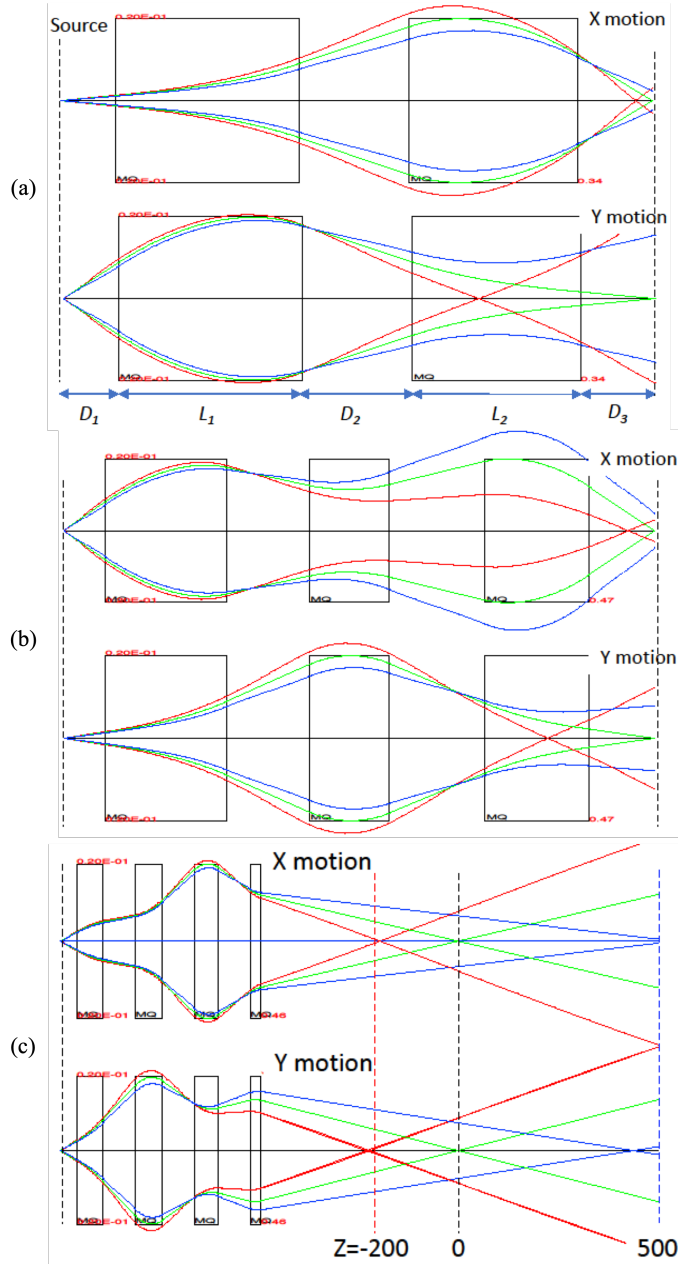


Fig. 2. The horizontal and vertical trajectories of particles with the maximum accepted angle in the doublet (a), triplet (b), and quartet (c) configurations. The beam moves from left to right. The different colors show the trajectories of similar particles with energies 20% above (blue) and 20% below (red) the nominal beam energy of 30 MeV (green). The main energy of the beam can be tuned by shifting the target location.

Alternatively, the target location can be moved to match the focal position of a particular beam energy as the focal positions of the quadrupoles are energy dependent. This scheme would only work for the quartet configuration, however, as any beam spot asymmetry grows worse the farther away from nominal focus.

The most effective way to tune and select the beam energy is by passing the beam through a magnetic dipole to disperse the beam depending on the particle energy, similar to a magnetic spectrometer. By adding an aperture at a certain deflection angle, only particles with the desired energy will make it through to the target. By chaining a series of dipoles together in a magnetic chicane or fragment separator type arrangement, the energy can be selected more precisely. Simulations were performed for these configurations but were not included in this presentation.

### C. 10 MeV Collimator at iP2

The first application experiment at iP2 is a radiobiological application utilizing 10 MeV proton beams, which requires a uniform dose distribution over a centimeter level at the sample location. Since oblique laser incidence on target [1] is planned, available space is limited further. In order to overcome constraints, a scheme with a compact collimating doublet with a dipole magnet is considered. A collimating doublet instead of a focusing doublet provides large beam size with the minimal real estate. A dipole was used to prevent neutrons and X-Rays from reaching to the samples [15]. The PMQ geometries and field strengths were also optimized to maximize collection efficiency and are shown in Fig. 3 and Table IV.

TABLE IV  
PROPERTIES OF THE PMQs FOR 10 MEV COLLIMATOR

	PMQ1	PMQ2
Inner radius (mm)	5	15
Outer radius (mm)	15	45
Gradient (T/m)	250	67
Effective length (mm)	50	50
Integrated Field Strength (T)	12.3	3.35

The dipole was positioned 1.5 m downstream of the second quadrupole to balance the charge density and uniformity. As the configuration consists of a doublet, it produces an asymmetric beam spot. To remedy this, the dipole would be oriented in a way to provide a kick perpendicular to the flat beam to "spread out" the dose distribution. This scheme is illustrated in Fig. 3. This design can provide a compact and cost-effective beam transport for radiobiological applications.

## IV. CONCLUSION

This paper explored various compact beam transport designs utilizing permanent magnets. This study has built a strong framework that allows the BELLA Center to swiftly model and adapt the beamline to new experimental requirements and requests from users of the facility. The iP2 beamline is ready to house various application experiments and furthermore, those

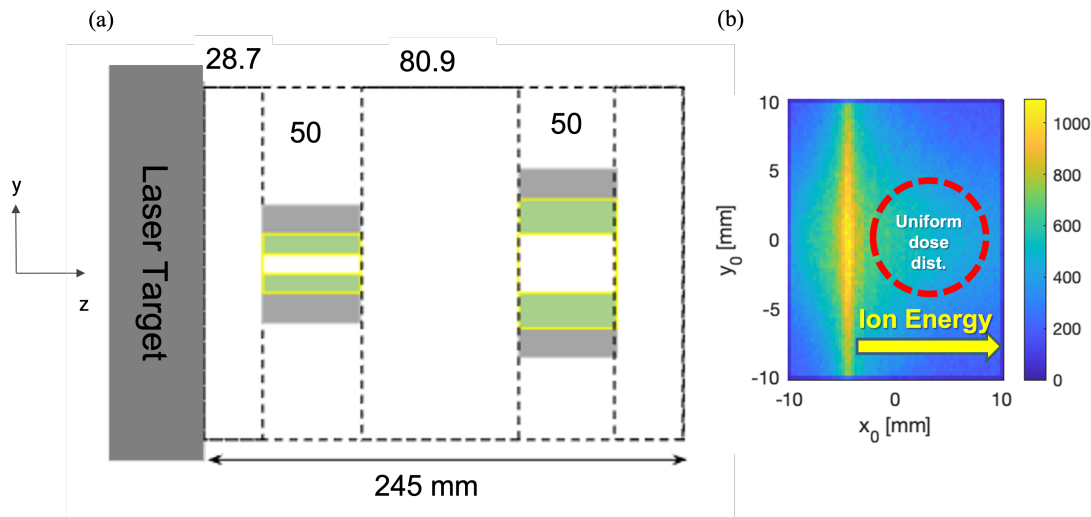


Fig. 3. (a) 10 MeV Collimator magnet geometry (dipole not shown). (b) Charge distribution (arbitrary units) at the proton sample location. A region of relatively uniform dose is achieved to the side from where the beam is focused.

designs can be used in any other facilities especially where a compact beam transport system is desired.

#### ACKNOWLEDGMENT

Authors would like to thank Sven Steinke for his contributions to the iP2 beamline.

#### REFERENCES

- [1] S. Hakimi, L. Obst-Huebl, K. Nakamura, A. Huebl, S. Bulanov, A. Jewell, and et al., “Newly commissioned ip2 beamline of the bella pw facility for investigation of high intensity laser-solid interactions,” *This proceedings*, 2023.
- [2] A. Macchi, M. Borghesi, and M. Passoni, “Ion acceleration by superintense laser-plasma interaction,” *Rev. Mod. Phys.*, vol. 85, pp. 751–793, May 2013.
- [3] S. V. Bulanov and V. S. Khoroshkov, “Feasibility of using laser ion accelerators in proton therapy,” *Plasma Physics Reports*, vol. 28, pp. 453–456, May 2002.
- [4] P. K. Patel, A. J. Mackinnon, M. H. Key, T. E. Cowan, M. E. Foord, M. Allen, D. F. Price, H. Ruhl, P. T. Springer, and R. Stephens, “Isochoric heating of solid-density matter with an ultrafast proton beam,” *Phys. Rev. Lett.*, vol. 91, p. 125004, Sep 2003.
- [5] T. Burris-Mog, K. Michel, F. Nürnberg, S. Busold, M. Bussmann, O. Deppert, G. Hoffmeister, M. Joost, M. Sobiella, Tauschwitz, B. Zielbauer, V. Bagnoud, T. Herrmannsdoerfer, M. Roth, and T. Cowan, “Laser accelerated protons captured and transported by a pulse power solenoid,” *Physical Review Special Topics - Accelerators and Beams*, vol. 14, pp. 7–13, 12 2011.
- [6] D. Jahn, D. Schumacher, C. Brabetz, J. Ding, S. Weih, F. Kroll, F. Brack, U. Schramm, A. Blažević, and M. Roth, “First application studies at the laser-driven light beamline: Improving proton beam homogeneity and imaging of a solid target,” *Nuclear Instruments and Methods in Physics Research Section A: Accelerators, Spectrometers, Detectors and Associated Equipment*, vol. 909, pp. 173 – 176, 2018. 3rd European Advanced Accelerator Concepts workshop (EAAC2017).
- [7] W. K. H. Panofsky and W. R. Baker, “A focusing device for the external 350-mev proton beam of the 184-inch cyclotron at berkeley,” *Review of Scientific Instruments*, vol. 21, no. 5, pp. 445–447, 1950.
- [8] J. van Tilborg, S. Steinke, C. G. R. Geddes, N. H. Matlis, B. H. Shaw, A. J. Gonsalves, J. V. Huijts, K. Nakamura, J. Daniels, C. B. Schroeder, C. Benedetti, E. Esarey, S. S. Bulanov, N. A. Bobrova, P. V. Sasorov, and W. P. Leemans, “Active plasma lensing for relativistic laser-plasma-accelerated electron beams,” *Phys. Rev. Lett.*, vol. 115, p. 184802, Oct 2015.
- [9] C. A. Lindström, E. Adli, G. Boyle, R. Corsini, A. E. Dyson, W. Farabolini, S. M. Hooker, M. Meisel, J. Osterhoff, J.-H. Röckemann, L. Schaper, and K. N. Sjobak, “Emittance preservation in an aberration-free active plasma lens,” *Phys. Rev. Lett.*, vol. 121, p. 194801, Nov 2018.
- [10] J. K. Lim, P. Frigola, G. Travish, J. B. Rosenzweig, S. G. Anderson, W. J. Brown, J. S. Jacob, C. L. Robbins, and A. M. Tremaine, “Adjustable, short focal length permanent-magnet quadrupole based electron beam final focus system,” *Phys. Rev. ST Accel. Beams*, vol. 8, p. 072401, Jul 2005.
- [11] T. Eichner, F. Grüner, S. Becker, M. Fuchs, D. Habs, R. Weingartner, U. Schramm, H. Backe, P. Kunz, and W. Lauth, “Miniature magnetic devices for laser-based, table-top free-electron lasers,” *Phys. Rev. ST Accel. Beams*, vol. 10, p. 082401, Aug 2007.
- [12] M. Nishiuchi, H. Sakaki, T. Hori, P. R. Bolton, K. Ogura, A. Sagisaka, A. Yogo, M. Mori, S. Orimo, A. S. Pirozhkov, I. Daito, H. Kiriya, H. Okada, S. Kanazawa, S. Kondo, T. Shimomura, M. Tanoue, Y. Nakai, H. Sasao, D. Wakai, H. Daido, K. Kondo, H. Souda, H. Tongu, A. Noda, Y. Iseki, T. Nagafuchi, K. Maeda, K. Hanawa, T. Yoshiyuki, and T. Shirai, “Measured and simulated transport of 1.9 mev laser-accelerated proton bunches through an integrated test beam line at 1 hz,” *Phys. Rev. ST Accel. Beams*, vol. 13, p. 071304, Jul 2010.
- [13] J. Bin, K. Allinger, W. Assmann, G. Dollinger, G. A. Drexler, A. A. Friedl, D. Habs, P. Hinz, R. Hoerlein, N. Humble, S. Karsch, K. Khrennikov, D. Kiefer, F. Krausz, W. Ma, D. Michalski, M. Molls, S. Raith, S. Reinhardt, B. Röper, T. E. Schmid, T. Tajima, J. Wenz, O. Zlobinskaya, J. Schreiber, and J. J. Wilkens, “A laser-driven nanosecond proton source for radiobiological studies,” *Applied Physics Letters*, vol. 101, no. 24, p. 243701, 2012.
- [14] J. Schreiber, M. Kaluza, F. Grüner, U. Schramm, B. M. Hegelich, J. Cobble, M. Geissler, E. Brambrink, J. Fuchs, P. Audebert, D. Habs, and K. Witte, “Source-size measurements and charge distributions of ions accelerated from thin foils irradiated by high-intensity laser pulses,” *Applied Physics B*, vol. 79, pp. 1041–1045, Dec 2004.
- [15] J. Bin, L. Obst-Huebl, J.-H. Mao, K. Nakamura, L. D. Geulig, H. Chang, Q. Ji, L. He, J. De Chant, Z. Kober, and et al., “A new platform for ultra-high dose rate radiobiological research using the bella pw laser proton beamline,” *Scientific Reports*, vol. 12, no. 1, 2022.
- [16] J. H. Bin, W. J. Ma, K. Allinger, H. Y. Wang, D. Kiefer, S. Reinhardt, P. Hinz, K. Khrennikov, S. Karsch, X. Q. Yan, F. Krausz, T. Tajima, D. Habs, and J. Schreiber, “On the small divergence of laser-driven ion beams from nanometer thick foils,” *Physics of Plasmas*, vol. 20, no. 7, p. 073113, 2013.
- [17] A. Macchi, M. Borghesi, and M. Passoni, “Ion acceleration by superintense laser-plasma interaction,” *Rev. Mod. Phys.*, vol. 85, pp. 751–793, May 2013.

- [18] K. Halbach, "Design of permanent multipole magnets with oriented rare earth cobalt material," *Nuclear Instruments and Methods*, vol. 169, no. 1, pp. 1–10, 1980.
- [19] W. Wan, L. Brouwer, S. Caspi, S. Prestemon, A. Gerbershagen, J. M. Schippers, and D. Robin, "Alternating-gradient canted cosine theta superconducting magnets for future compact proton gantries," *Phys. Rev. ST Accel. Beams*, vol. 18, p. 103501, Oct 2015.
- [20] O. Chubar, P. Elleaume, and J. Chavanne, "A three-dimensional magnetostatics computer code for insertion devices," *Journal of Synchrotron Radiation*, vol. 5, pp. 481–484, May 1998.
- [21] M. B. Kyoko Makino, "Cosy infinity version 9," *Nuclear Instruments and Methods*, vol. A558, pp. 346–350, 2005.